IS SCATTERING OR REFLECTION MORE EFFECTIVE IN CAUSING BOUNDARY MIXING?

Naihuai Xu and Peter Müller

Department of Oceanography, University of Hawaii, 1000 Pope Road, Honolulu HI 96822

Abstract

Comparison is made of the redistributed energy flux resulting from scattering of two-dimensional internal waves off one-dimensional random topography with that resulting from the reflection of two-dimensional internal waves off a straight slope. Reflection redistributes much more energy flux than scattering does (2.86 mW m^{-2} as opposed to 0.99 mW m^{-2}), but reflection redistributes less energy flux to high wavenumbers than does scattering (0.90 mW m^{-2} as against 0.97 mW m^{-2} to wavenumbers greater than 10^{-4} cpm). Scattering might thus be equally or more efficient than reflection in causing high shears and mixing near the bottom.

1. Introduction

Boundary mixing has been advocated (e.g., Ivey, 1987) as a process responsible for diapycnal mixing in the deep ocean. Diapycnal mixing is required to satisfy the global balances of mass and heat and to support observed poleward heat transport. Internal wave reflection at topography has been proposed (Eriksen, 1982, 1985; Garrett and Gilbert, 1988) to cause this boundary mixing. Recently, Xu (1991) and Müller and Xu (1991) have suggested scattering at random topography. Internal wave interaction with topography distorts the wave spectrum and redistributes the incoming energy flux within the wavenumber space. Waves scattered or reflected to high wavenumbers might break and cause boundary mixing.

The reflection process has been intensively studied by Eriksen (1982, 1985) and Garrett and Gilbert (1988). When the incident wave length is much shorter than the radius of curvature of topography, internal waves can be treated as encountering an infinite flat slope. The reflection process conserves the frequency and the tangential component of the wavenumber vector. Eriksen (1982, 1985) calculated the absolute difference between the incident and reflected energy flux which is comparable to the incident flux. This quantity does not tell how much energy flux could be used for generating shears, but can serve as the upper limit. In an attempt to assess quantitatively how much energy flux is available for mixing, Garrett and Gilbert (1988) assumed that waves with mode numbers greater than a critical mode number undergo instability, break, and cause mixing. This critical mode number is determined by assuming that waves with mode numbers larger than the critical number cause the inverse Richardson number to become larger than one. Given typical parameters for the deep ocean, the energy flux available for mixing is about 0.25 $\mathrm{mW\,m^{-2}}$ (about 1.4% of incident flux), much smaller than absolute energy flux difference calculated by Eriksen (1985).

Scattering of internal waves at a random topography was theoretically analyzed by Müller and Olbers (1975) in the Bragg scattering or weak interaction limit. Olbers and Pomphrey (1981) estimated the redistributed energy flux in this limit and found it to be as small as $\sim 10^{-2} - 10^{-3}$ of the incident one. The energy flux available for mixing should be even smaller than this. However, the formula used to calculate the redistributed energy flux contains an algebraic error. Rubenstein (1988) treated a simplified problem: a two-dimensional wavefield interacting with one-dimensional topography. In a detailed study, he found significant energy flux transfer by assuming that the probability of scattering from an incident wavenumber to a scattered wavenumber is proportional to the ratio of the respective fluxes. Unfortunately, he interpreted this probability as a density in a vertical wavenumber space whereas it is a probability in horizontal wavenumber space. A systematic derivation and evaluation of the scattering integral is given in Xu (1991) and Müller and Xu (1991). Here we compare the scattering and reflection processes and concentrate on the question of which process is more efficient in causing boundary mixing, scattering or reflection.

We emphasize here the difference between the redistributed energy flux and the energy flux available for mixing. The redistributed flux represents the energy flux that is transferred to other wavenumbers, either lower or higher. When the energy flux is redistributed to lower wavenumbers, the field becomes more stable. The shear in the field decreases. This process does not favor mixing. On the other hand, if wave energy flux is transferred to higher wavenumbers, shear is increased and the flow field tends to be less stable and more prone to breaking. This process favors mixing. The energy flux available for mixing is the energy flux to high wavenumbers, which causes the shear to become larger than critical. This energy flux will drive the field to instability, and breaking of internal waves thus occurs.

2. Scattering process

We consider the simplified model of two-dimensional internal waves scattered off one-dimensional random topography or reflected off a straight slope.

Baines (1971) considered the two-dimensional internal wave interaction with an arbitrary flat bump topography. The slope of the flat bump topography is required to be less than the slope of the group velocity. The radiation condition was formulated as a homogeneous integral equation. An incident wave impinging on this topography will generate a forward transmitted wave and a backward reflected wave. The solution to the system is obtained by solving a Fredholm integral equation of the second kind. If we further assume that the vertical wavelength of an incident wave is much smaller than the height of topography (the ratio of them is a small parameter ε_1), the Fredholm integral equation can be solved to the second order of ε_1 so that we can obtain the lowest order corrections of the scattered energy flux. The redistributed energy flux is then (Xu, 1991)

$$\begin{aligned} D^s(\omega,\alpha) &= \int_0^\infty d\alpha' \mu^2 V(\omega)[E(\omega,\alpha')\alpha - E(\omega,\alpha)\alpha'] \\ &\quad [S_1(\alpha+\alpha') + S_1(\alpha-\alpha')] \end{aligned} \tag{1}$$

where $E(\omega,\alpha)$ is the incident energy density spectrum, $S_1(\alpha)$ the topography height spectrum, $V(\omega)/\alpha$ the vertical group velocity, $\mu^2 = (N^2-\omega^2)/(\omega^2-f^2)$, α the modulus of horizontal wavenumber and ω the wave frequency. For each frequency, the energy flux is conserved, i.e., $\int D^s(\omega,\alpha)d\alpha = 0$. This can be seen from the antisymmetric character of

$$[E(\omega,\alpha')\alpha - E(\omega,\alpha)\alpha']. \tag{2}$$

The redistributed energy flux consists of two parts: the first part is the gain of energy flux at α from interaction of incident wavenumber α' with topographic wavenumber $\alpha \pm \alpha'$. More energy flux is gained at the higher wavenumbers than at the lower wavenumbers. This can be seen by looking at the first part of D^s denoted by $D^s_{11}(\omega,\alpha)$. Using k_1' to represent the horizontal wavenumber of an incident wave and k_1'' the topographic wave, then $D^s_{11}(\omega,\alpha)$ can be transformed as

$$\begin{aligned} D^s_{11}(\omega,\alpha) &= D^s_{11}(\omega,|k_1'+k_1''|) \\ &= \int_{-\infty}^\infty dk_1' \mu^2 V(\omega) E(\omega,k_1')|k_1'+k_1''| S_1(k_1'') \end{aligned} \tag{3}$$

where $\alpha = |k_1'+k_1''|$. The transfer function is proportional to α. The scattered wave energy flux will be larger for a high scattered wavenumber α than for low scattered wavenumber α. The second term of Eq. (1) acts like a friction to the incident energy flux. Waves that would be reflected to a certain wavenumber α are scattered to another wavenumber α'. Scattering always transfers energy flux to high wavenumbers. This result can be understood using statistical mechanics and the H-theorem (Müller and Xu, 1991).

Equation (1) can be derived by several approaches (see Xu, 1991). Rubenstein's hypothetical approach differs by a factor of μ and exaggerates the scattering efficiency at low frequencies. This extra factor results from interpreting a probability density with respect to horizontal wavenumber as a density with respect to vertical wavenumber.

3. Reflection process

The two-dimensional internal wave reflection off a straight slope is considered here. Assume that the flat slope $z = sx$ lies in the $x - z$ plane where $s = \tan \varphi_o$, the inclination of the topography relative to the horizontal plane. The reflected wavenumber vector is denoted as $\vec{k} = (k \cos \theta, 0, k \sin \theta)$, $\alpha = |k \cos \theta|$. The inclination θ is determined by the frequency and radiation condition. The reflection law requires that the frequency and tangential component of wavenumber vector conserves in the reflection. The reflected energy spectrum in wavenumber space under the constraint of radiation and boundary conditions (no normal flow across the boundary) yields

$$E_r(\vec{k}) = E(\vec{k^i}) \tag{4}$$

where $\vec{k^i}$ is the incident wavenumber vector. It shows that in the case of reflection, the energy density spectrum at the reflected and incident wavenumber are the same. This conclusion is consistent with Eriksen's results (1982, 1985). Under the constraint of the radiation condition, incident waves exist in only certain permissible regions shown in Figure 1. For each frequency, there are two permissible incident wavenumbers, one of them is in the first quadrant, the other is in another quadrant. If the incident wavenumbers lie in the first quadrant of the $k_1 - k_3$ plane, the reflected horizontal wavenumbers are always greater than the corresponding incident ones, while if the incident wavenumbers are in any other quadrant, the reflected horizontal wavenumbers will be smaller than the corresponding incident ones. The energy flux at each frequency is therefore transferred to both high and low wavenumbers. The difference between the reflected and incident normal energy flux therefore is

$$D(\omega, \alpha) = \sum_{r=1}^{2} \left[E\left(\omega, \left| \frac{\alpha \cos(\theta_r - \varphi_o)}{\cos(\theta_r + \varphi_o)} \right| \right) - E(\omega, \alpha) \right] \frac{N^2 - f^2}{\omega \alpha} |\sin \theta_r \cos^2 \theta_r \cos(\theta_r + \varphi_o)|, \tag{5}$$

where θ_1 and θ_2 correspond to the two inclinations of the permissible reflected wavenumbers. The redistributed energy flux vanishes when integrated over all horizontal wavenumbers. At the critical frequency defined by

$$\omega_c^2 = N^2 \sin \varphi_o + f^2 \cos^2 \varphi_o, \tag{6}$$

one of the reflected wavenumbers ($\theta = \pi/2 + \varphi_o$) becomes infinity, the other one ($\theta = -\pi/2 - \varphi_o$) goes to zero. This implies that the energy flux is redistributed to

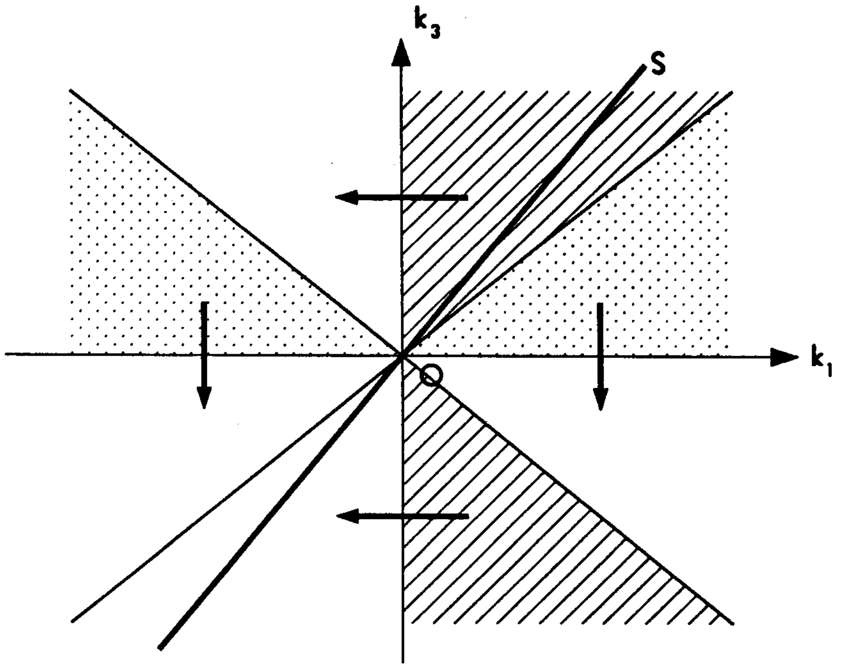

Figure 1: Regions of permissible incident and reflective waves in the horizontal-vertical wavenumber plane. The heavy solid straight line represents the bottom slope. The light solid lines represent the critical frequency cone. The cross-hatched and stippled regions are permissible incident wavenumbers. For the cross-hatched regions the reflection is subcritical, for the stippled region the reflection is supercritical. The incident wavenumbers reflect to regions are indicated by the arrows.

very high and low wavenumbers at the critical frequency.

4. Background Spectra

For analytical convenience, we choose the Garrett and Munk model GM76 (Desaubies, 1976)

$$E(\omega,\alpha) = b^2 N N_0 E_0 B(\omega) \frac{A(\alpha/\alpha_*)}{\alpha_*} \tag{7}$$

where

$$B(\omega) = \frac{2}{\pi}\frac{f}{\omega}(\omega^2 - f^2)^{-1/2} \tag{8}$$

$$A(\lambda) = \frac{2}{\pi}(1+\lambda^2)^{-1} \tag{9}$$

and $N_o = 5.2 \times 10^{-3} s^{-1}$, $E_o = 6 \times 10^{-5}$ and $b = 1.3 \times 10^3$ m. The bandwidth is given by

$$\alpha_*(\omega) = \left(\frac{\omega^2 - f^2}{N_o^2 - \omega^2}\right)^{1/2} \frac{\pi}{b} j_*, \tag{10}$$

here $j_* = 3$ is the frequency-independent equivalent mode number bandwidth. We set the high wavenumber cutoff

$$\alpha_{hc}(\omega) = \left(\frac{\omega^2 - f^2}{N^2 - \omega}\right)^{1/2} \beta_{hc}, \tag{11}$$

where $b_{uc} = 0.1$ cpm. Finite incident energy flux is achieved by assuming the lower wavenumber cutoff

$$\alpha_{lc}(\omega) = \lambda_l \alpha_* \tag{12}$$

where $\lambda_l \approx 0.154$ based on identical energy fluxes in both the continuous GM76 and the discrete GM81 (Munk, 1981) models.

The bottom spectrum is chosen as formulated by Bell (1975)

$$S_1(\alpha) = \tilde{F}_o \tilde{S}_1(k_1) \tag{13}$$

where $\tilde{F}_o = 0.5\pi F_o/\alpha_o = 2.0 \times 10^4 \pi^3$ cpm^{-2} is the variance and

$$\tilde{S}_1(k_1) = \begin{cases} \frac{\alpha\alpha_1}{(\alpha^2+\alpha_1^2)^{3/2}} & \text{for } k_1 < \alpha_c^t \\ 0 & \text{for } k_1 > \alpha_c^t \end{cases} \tag{14}$$

describes the variation, the high wavenumber cutoff is α_c^t. The rms height of this spectrum is about 125 m.

In addition, we assume the parameters for typical deep ocean conditions are $f = 0.042$ cph (mid-latitude, 30°), $N = 0.4$ cph and $\varphi_o = 4°$ corresponding to $s = \tan\varphi_o = 0.07$.

5. Comparison of redistributed energy fluxes by scattering and reflection

With a specified interior internal wave spectrum and a topographic spectrum, we can evaluate the redistributed energy flux spectrum for each process.

Figure 2 shows the comparison of the redistributed energy fluxes $D(\omega, \alpha)$ as a function of α for frequency $\omega = 1.33f$ in a variance conserving representation. In the scattering process, energy flux is redistributed from low to high wavenumbers,

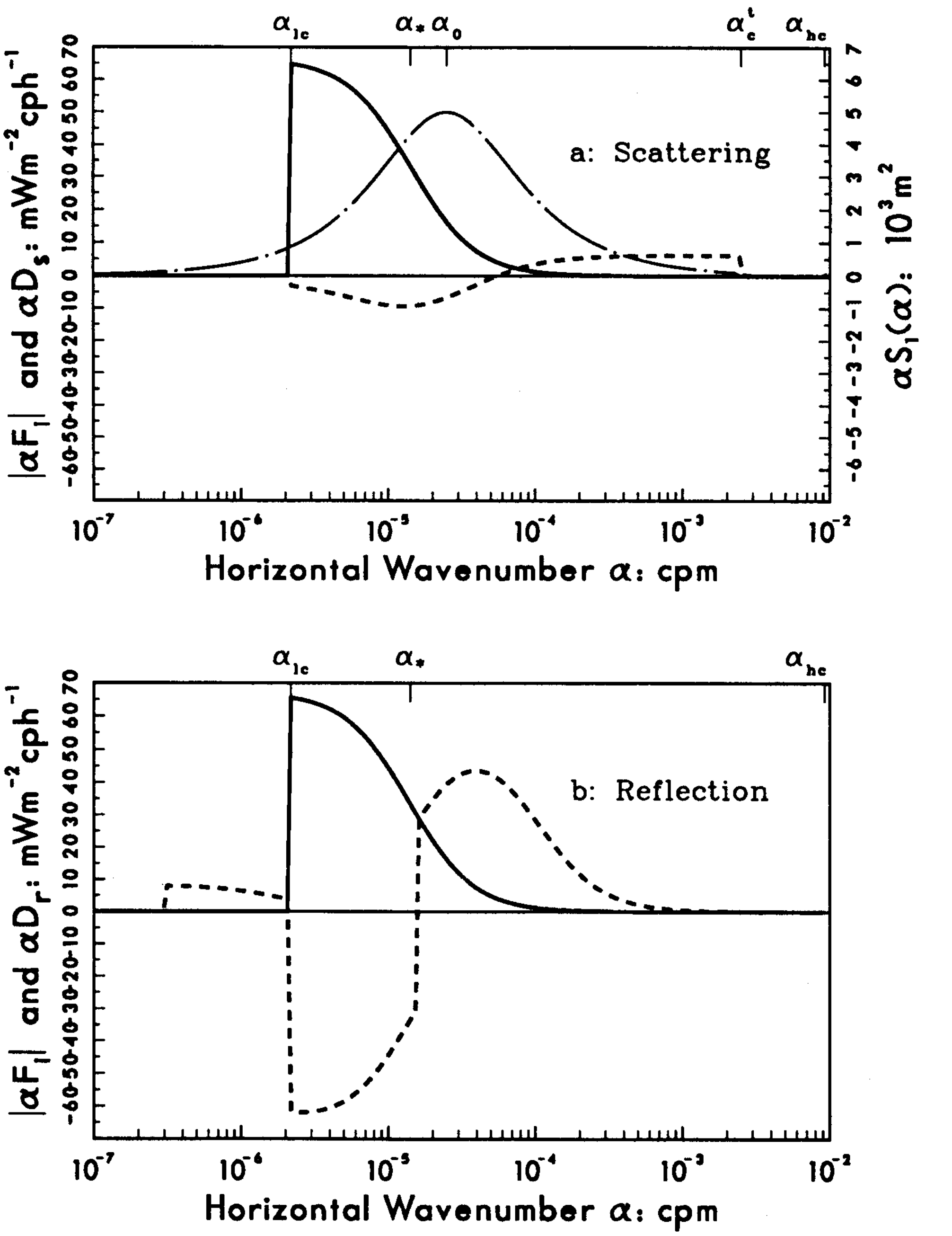

Figure 2: Comparison of redistributed energy fluxes $D(\omega, \alpha)$ by scattering or reflection. Incident energy flux $|F_i(\alpha, \omega)|$ (solid line) and redistributed energy flux $D(\alpha, \omega)$ (dashed line) as a function of horizontal wavenumber for frequency $\omega = 1.33f$. The representation is variance conserving. The wavenumbers α_{lc}, α_*, and α_{hc} are the low wavenumber cutoff, the bandwidth, and the high wavenumber cutoff of the incident internal wave spectrum, respectively. (a). For two-dimensional internal wave scattering model. $S_1(\alpha)$ (dash-dotted line) is the bottom spectrum. The wavenumber α_o and α_c^t are the bandwidth and high wavenumber cutoff of the topographic spectrum, respectively. (b). For two-dimensional internal wave reflection model. The bottom slope is $\gamma = 0.07$ and the critical frequency is $\omega_c = 1.2f$.

whereas in the reflection process energy flux is transferred from medium to both high and low wavenumbers. Because of no normal flow across the boundary, the area of negative lobes equals the area of positive lobes.

Integration with respect to wavenumber α yields the redistributed energy flux

$$D^{+}(\omega) = \frac{1}{2}\int d\alpha |D(\omega, \alpha)| \qquad (15)$$

as shown in Figure 3. The total redistributed energy flux D^{+} is 3.89 $\mathrm{mW\,m^{-2}}$ out of 18.2 $\mathrm{mW\,m^{-2}}$, the incident normal energy flux, for the reflection process, and 1.2 $\mathrm{mW\,m^{-2}}$ out of 17.6 $\mathrm{mW\,m^{-2}}$ for the scattering process. The reflection process redistributes 21% of the incident energy flux as against 6.8% for the scattering process. Reflection is much more efficient than scattering in redistributing energy flux. Scattering redistributes most of the energy flux near the inertial frequency, reflection around the critical frequency.

An important difference between the two processes is the frequency-integrated energy flux spectrum $D(\alpha)$ as shown in Figure 4. The reflection process

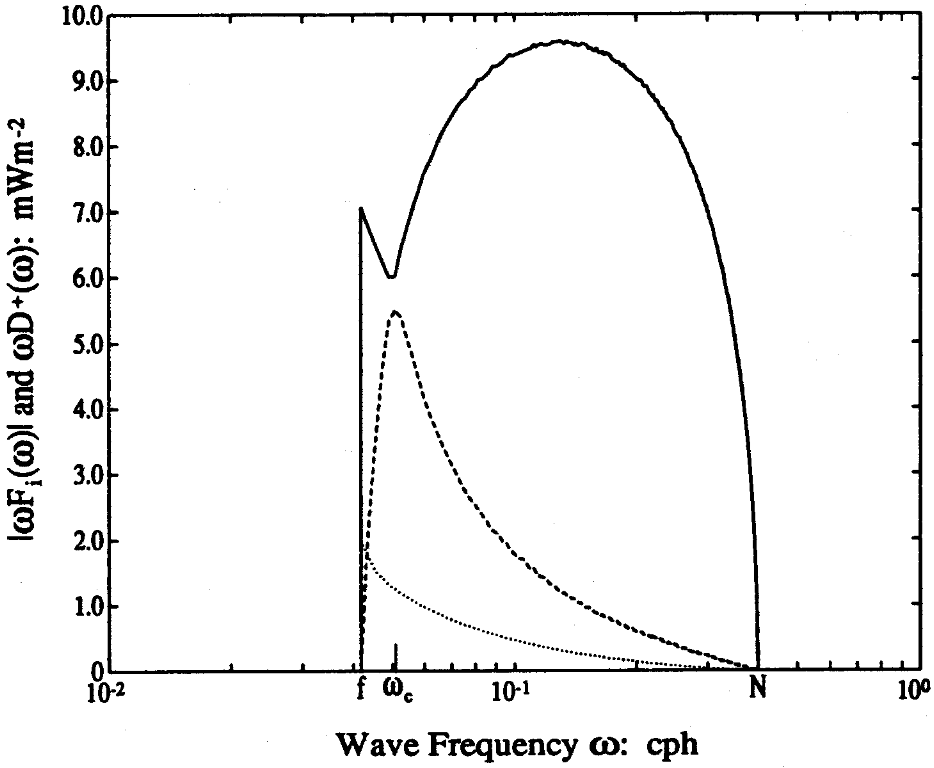

Figure 3: Comparison of two-dimensional scattering and reflection. Incident energy flux $|F_i(\omega)|$ (solid line), redistributed energy flux $D^{+}(\omega)$ by scattering (dashed line) and redistributed energy flux $D^{r}(\omega)$ by reflection (dotted line) as a function of frequency in a variance-conserving representation.

redistributes 2.86 $\mathrm{mW\,m^{-2}}$ of incoming energy flux (15.7% incident), scattering redistributes 0.99 $\mathrm{mW\,m^{-2}}$ (5.6% incident). These numbers are smaller than the integrated D^+ since contributions cancel by frequency integration. The scattering process redistributes energy flux to much higher wavenumbers. In the scattering process 0.97 $\mathrm{mW\,m^{-2}}$ out of 0.99 $\mathrm{mW\,m^{-2}}$, the total redistributed energy flux is transferred to high wavenumbers above 10^{-4} cpm, whereas in the reflection process, 0.90 $\mathrm{mW\,m^{-2}}$, which is less than 32% of the total redistributed energy flux, is moved to wavenumbers above 10^{-4} cpm. Scattering hence must be more efficient than critical reflection in increasing the shear and the inverse Richardson number near the bottom.

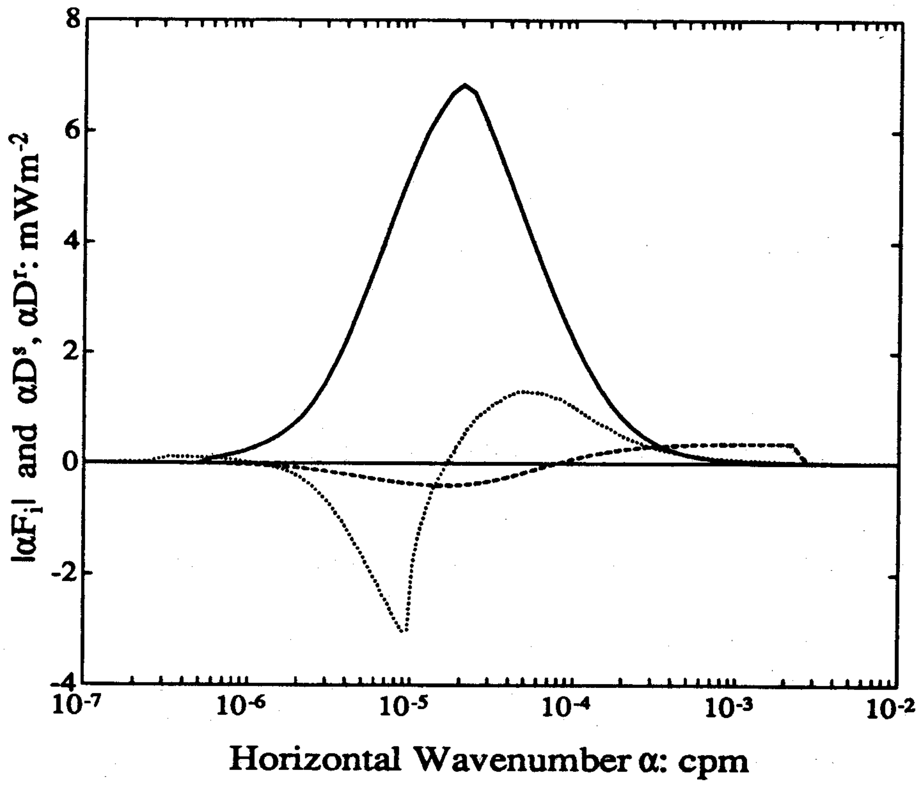

Figure 4: Comparison of two-dimensional scattering and reflection. Incident energy flux $|F_i(\alpha)|$ (solid line), energy flux $D^s(\alpha)$ redistributed by scattering (dashed line), and energy flux $D^r(\alpha)$ redistributed by reflection (dotted line) in a variance conserving representation.

6. Discussions

Here we discuss some possible restrictions:

Three-dimensional scattering model

Are the conclusions drawn from the comparison of scattering and reflection processes for the two-dimensional geometry still valid for three-dimensional model? Müller and Xu's (1991) and Xu's (1991) studies show that the two-dimensional model is a good representation of the three-dimensional internal wave interaction model in terms of the redistributed energy flux and other quantities. Using the perturbation method, Xu (1991) and Müller and Xu (1991) obtain a similar result to Eq. (16) for the redistributed energy flux

$$\begin{aligned} D^s(\omega,\vec{\alpha}) &= 2\int_{-\infty}^{\infty} d^2\vec{\alpha}_1 \frac{\mu^2}{\alpha^2\alpha_1^2} V(\omega)|\vec{\alpha}_1\cdot\vec{\alpha}_1 + i\frac{\vec{f}}{\omega}\cdot\vec{\alpha}\times\vec{\alpha}_1|^2 \\ & [E(\omega,\vec{\alpha}_1)\alpha - E(\omega,\vec{\alpha}_1)\alpha_1] S_2(\vec{\alpha}-\vec{\alpha}_1), \end{aligned} \tag{16}$$

where $S_2(\vec{\alpha})$ is the two-dimensional random topography spectrum. $S_2(\alpha)$ is derived as

$$S_2(\alpha) = \frac{\tilde{F}_o \alpha_o \alpha}{(\alpha^2+\alpha_o^2)^{3/2}}, \tag{17}$$

a natural extension of one-dimensional bottom topography by the assumption of horizontal isotropy, and $E(\omega,\vec{\alpha})$ is specified as GM76 as before.

Numerical evaluation of Eq. (16) gives similar features as shown for the two-dimensional model in Figures 2, 3, and 4. Magnitudes differ only slightly by less than 15% of the corresponding two-dimensional model results. The total redistributed energy flux for the three-dimensional model is 1.14 $\mathrm{mW\,m^{-2}}$ as opposed to 0.99 $\mathrm{mW\,m^{-2}}$ for the two-dimensional case. The gain part of the redistributed energy flux is dominant at high horizontal wavenumbers and the lost part at lower horizontal wavenumbers. With this approximation, Eq. (16) can be integrated to yield

$$D(\omega,\alpha) \approx 2\frac{N^2-\omega^2}{\omega^2-f^2}\frac{1}{2}\frac{\omega^2+f^2}{\omega^2}V(\omega)[\alpha E(\omega)S_2(\alpha) - E(\omega,\alpha)C] \tag{18}$$

where $E(\omega) = \int d\alpha E(\omega,\alpha)$ and

$$C = \int d^2\alpha\alpha S_2(\alpha) = \tilde{F}_o\alpha_o\{\ln\frac{2\alpha_c^t}{\alpha_o} - 1\}. \tag{19}$$

This approximation turns out to be a good one; it is indistinguishable from the numerically evaluated solution plotted in Figure 2. The approximation (18) is particularly useful in theoretical study to derive the quantities associated with the three-dimensional internal wave scattering model.

Limits of the scattering theory

For the establishment of both three-dimensional and two-dimensional internal wave scattering theory, an expansion is made in which two parameters are assumed small: ε_1 is the ratio of topography height to the incident vertical internal wavelength, ε_2 is the ratio of the slope of topography to the slope of wave rays, in the root mean square sense. The GM spectrum implies the variance of β

$$\langle \beta^2 \rangle \approx \beta_* b_{uc} = \left(\frac{2\pi}{1000 \text{ m}} \right)^2 \frac{N}{N_o}. \tag{20}$$

With the specified topographic spectrum S_2, we obtain

$$\varepsilon_1 = 2\pi \frac{125}{100} \left(\frac{N}{N_o} \right)^{1/2} \tag{21}$$

which is of order one for the deep ocean where $N/N_o \sim 10^{-1}$. Bell's spectrum implies a slope variance of

$$\gamma^2 = \int d\alpha S_2(\alpha)\alpha^2 = \tilde{F}_o \alpha_o \alpha_c^t \approx (0.2)^2, \tag{22}$$

hence

$$\varepsilon_2 = 0.2 \left(\frac{N^2 - \omega^2}{\omega^2 - f^2} \right)^{1/2} \tag{23}$$

which is larger than one for $\omega \leq 2f$. For typical ocean conditions, the expansion is only marginally correct and breaks down for near inertial oscillation. The transfer to high wavenumber is a general tendency not limited to weak interaction. It represents the approach to statistical equilibrium. Since the approach to equilibrium is generally faster the larger the nonlinearities are, our results can be expected to represent a lower bound.

Singularities in solutions:

Singularities might indicate possible breakdowns of the theory and therefore deserve careful study. In horizontal wavenumber space $\alpha \to 0$ and $\alpha \to \infty$ represent singularities causing the energy flux and energy density to become infinite. These singularities are overcome by assuming low and high wavenumber cutoffs. There still exist singularities in wave frequency. For the scattering process the energy density has a nonintegratable singularity but energy flux is finite. The reflected energy density spectrum at one of the critical angles $\theta = \pi/2 + \varphi_o$ (corresponding to the critical frequency ω_c) has a nonintegrable singularity. The reflected energy flux spectrum is finite here and has the greatest contribution to the total reflected energy flux spectrum. This ensures that none of the frequencies become the singular point of scattered or reflected energy fluxes.

Energy flux available for mixing:

The essential quantity in causing boundary mixing is the redistributed energy flux available for mixing. For the typical parameters of ocean conditions specified in this paper, Garrett and Gilbert's (1988) results show that the energy flux available for mixing is about 0.25 $\mathrm{mW\,m^{-2}}$ and is due to the redistributed energy flux with wavenumbers beyond $\alpha_c \approx 2 \times 10^{-4}$ cpm for the three-dimensional internal wave reflection model. Using the Eq. (18) to estimate the corresponding energy flux available for mixing for the three-dimensional internal wave scattering model, we find about 0.80 $\mathrm{mW\,m^{-2}}$ of the redistributed energy flux will go to mixing.

7. Conclusions

Both scattering of internal waves off random topography (Müller and Olbers, 1975; Olbers and Pomphrey, 1981; Rubenstein 1988, Müller and Xu, 1991 and Xu, 1991) and reflection of internal waves off a straight slope (Eriksen, 1982 and 1985; Garrett and Gilbert, 1988) have been carefully studied. Here we assessed whether scattering or reflection is the more efficient process in causing boundary mixing?

In order to answer this question, we compared scattering and reflection together for the two-dimensional internal wave models. The scattering of three-dimensional internal waves off two-dimensional random topography is more realistic. The study shows that the simplified two-dimensional internal wave scattering model is a good approximation to this general three-dimensional scattering model. They show almost similar features and only differ slightly in magnitudes-by less than 15% in terms of redistributed energy flux. The conclusions are still valid for the general model of three-dimensional internal wave interactions. The scattering process is analyzed under the assumptions of (i) the height of topography is smaller than the vertical wavelength and (ii) the slope of topography is smaller than the wave slope, in the root mean square sense. For typical deep ocean conditions, these conditions are only marginally satisfied, especially the slope condition, which breaks down for near inertial waves. The reflection theory presented here is consistent with Eriksen's work. Comparison between scattering and reflection processes is made in detail. In the reflection process, energy flux is redistributed to both high and low wavenumbers, whereas in the scattering process scattered energy flux is transferred to high wavenumbers. Reflection redistributed much more normal energy flux than the scattering process does (2.86 $\mathrm{mW\,m^{-2}}$ as opposed to 0.99 $\mathrm{mW\,m^{-2}}$), but the reflection process redistributes less energy flux to high wavenumbers, for example, to $\alpha > 10^{-4}$ cpm, than the scattering process ($0.9\ \mathrm{mW\,m^{-2}}$ opposed to $0.97\ \mathrm{mW\,m^{-2}}$). Since most of the redistributed energy flux goes to high wavenumbers, we could roughly estimate the redistributed energy flux available for mixing as $0.80\ \mathrm{mW\,m^{-2}}$ compared with $0.25\ \mathrm{mW\,m^{-2}}$ estimated for the reflection process by Garrett and Gilbert (1988). Scattering might thus be equally or more efficient than the reflection in causing shears and mixing near the bottom.

Acknowledgments

This work relates to Department of Navy Grant N00014-89-J-1315 issued by the Office of Naval Research. The United States Government has a royalty-free license throughout the world in all copyrightable material contained herein. This paper is School of Ocean and Earth Science and Technology contribution 2637.

References

Baines, P. G., 1971a: The reflexion of internal/inertial waves from bumpy surfaces, *J. Fluid Mech.*, 46, part 2, 273-291.

Bell, T. H., 1975: Statistical features of sea-floor topography, *Deep-Sea Res.*, 22, 883-892.

Desaubies, Y. J. F., 1976: Analytical representation of internal wave spectra, *J. Phys. Oceanogr.*, 6, 976-981.

Eriksen, C. C., 1982: Observations of internal wave reflection off sloping bottoms, *J. Geophys. Res.*, 87, 525-538.

Eriksen, C. C., 1985: Implications of ocean bottom reflection for internal wave spectra and mixing, *J. Phys. Oceanogr.*, 15, 1145-1156.

Garrett, C.J.R. and D. Gilbert, 1988: Estimates of vertical mixing by internal waves reflected off a sloping bottom, in *Small-scale turbulence and mixing in the ocean.* J. C. J. Nihoul and B. M. Jamart (editors), 405-424.

Ivey, G. N., 1987: The role of boundary mixing in the deep ocean, *J. Geophys. Res.*, Vol. 92, C11, 11,873-11,878.

Müller, P. and D. J. Olbers, 1975: On the dynamics of internal waves in the deep ocean, *J. Geophys. Res.*, Vol. 80, 3848-3860.

Müller, P. and N. Xu, 1991: Scattering of oceanic gravity waves off random bottom topography, submitted to *J. Phys. Ocean.*

Munk, W. H., 1981: Internal waves and small-scale processes, in *Evolution of Physical Oceanography Scientific Surveys in Honor of Henry Stommel*, edited by B. A. Warren and C. Wunsch, MIT Press, Cambridge, Mass., pp. 264-291.

Olbers, D. J. and N. Pomphrey, 1981: Disqualifying two candidates for the energy balance of oceanic internal waves, *J. Phys. Oceanogr.*, 11, 1423-1425.

Rubenstein, D., 1988: Scattering of inertial waves by rough bathymetry, *J. Phys. Oceanogr.*, 18, 5-18.

Xu, N., 1991: Interactions of internal waves with random bottom topography and a straight slope, M.S. thesis, Univ. of Hawaii.